

VARIABLE STARS IN THE FORNAX DSPH GALAXY.
II. PULSATING STARS BELOW THE HORIZONTAL BRANCH ¹

ENNIO PORETTI², GISELLA CLEMENTINI³, ENRICO V. HELD⁴, CLAUDIA GRECO^{3,5}, MARIO MATEO⁶, LUCA DELL'ARCIPRETE²,
LUCA RIZZI⁷, MARCO GULLIEUSZIK⁴, AND MARCELLA MAIO³

Revised version 3.0

ABSTRACT

We have carried out an intensive survey of the northern region of the Fornax dwarf spheroidal galaxy with the aim of detecting the galaxy's short-period pulsating stars ($P < 0.25$ days). Observations collected over three consecutive nights with the Wide Field Imager of the 2.2m MPI telescope at ESO allowed us to detect 85 high-amplitude (0.20–1.00 mag in B -light) variable stars with periods in the range from 0.046 to 0.126 days, similar to SX Phoenicis stars in Galactic metal-poor stellar populations. The plots of the observed periods vs. the B and V magnitudes show a dispersion largely exceeding the observational errors. To disentangle the matter, we separated the first-overtone from the fundamental-mode pulsators and tentatively identified a group of subluminous variables, about 0.35 mag fainter than the others. Their nature as either metal-poor intermediate-age stars or stars formed by the merging of close binary systems is discussed. The rich sample of the Fornax variables also led us to reconstruct the Period–Luminosity relation for short-period pulsating stars. An excellent linear fit, $M_V = -1.83(\pm 0.08) - 3.65(\pm 0.07) \times \log P_F$, was obtained using 153 δ Scuti and SX Phoenicis stars in a number of different stellar systems.

Subject headings: galaxies: distance and redshifts – galaxies: individual (Fornax) – δ Scuti – stars: variables: others – blue stragglers – techniques: photometric

1. INTRODUCTION

In globular clusters, the systematic detection of the short-period ($P < 0.25$ days) pulsating stars located below the horizontal branch (namely, SX Phe and δ Sct stars) started about twenty years ago (e.g., Mateo et al. 1988; Nemeč et al. 1995). At that time, Nemeč, Nemeč & Lutz (1994) listed 14 SX Phe stars in NGC 5053, ω Cen and NGC 5466. The use of these variable stars as distance indicators has made some progress in the last years (e.g., Pych et al. 2001; Mazur et al. 2003; Olech et al. 2005). However, due to their intrinsic faintness, not many of these pulsating stars have been discovered so far in stellar systems outside the Milky Way: Mateo et al. (1998) and Poretti (1999a) describe the first results obtained for SX Phe stars in the Carina dwarf spheroidal (dSph) galaxy; McNamara, Clementini & Marconi (2007) have used a sample of δ Sct stars to estimate the distance to the Large Magellanic Cloud. To exploit in a more complete way the potential of these variable stars as distance indicators and stellar population tracers we have carried out a search for pulsating stars below the horizontal branch as starting point for an extensive project on the Fornax dSph. This galaxy is an ideal target since:

(i) it is known to host a mix of old and intermediate-age stars with different metal abundances (see, e.g., Battaglia et al. 2006; Coleman & de Jong 2008, and refs. therein); (ii) its size and distance make the observation of large fractions of the galaxy, down to a limiting magnitude of about 3.0 mag below the horizontal branch, practical using a medium-class telescope equipped with a wide-field imager, using exposure times fully adequate to reveal the galaxy's short-period pulsators. Our project also allowed a more comprehensive study of several classes of variable stars in the Fornax dSph galaxy, and it was extended over the course of the years to cover the galaxy's field and its system of five globular clusters, through the acquisitions of new observations with other telescopes (Clementini et al. 2006; Greco et al. 2007).

The nomenclature of the short-period pulsating stars below the horizontal branch is confusing. In the Milky Way there is a physical distinction between δ Sct and SX Phe stars: the former are Population I stars (Pop. I), the latter are Population II (Pop. II) objects. Low-amplitude, nonradial modes are typical of the δ Sct stars, but intensive and accurate surveys in globular clusters have provided observational evidences that they are excited also in the SX Phe stars (Pych et al. 2001; Mazur et al. 2003; Olech et al. 2005). Therefore, the amplitude can vary from a few 0.001 mag to several 0.1 mag both in the δ Sct and in the SX Phe variables. The δ Sct stars showing amplitude larger than 0.20 mag are generally referred to as High-Amplitude δ Sct (HADS) stars. As in the case of high-amplitude SX Phe stars, the main pulsation period is a radial mode. The pulsation period can provide a rough separation between HADS and SX Phe stars, since periods of HADS vary from 0.07 to 0.25 days (Poretti 2001), while most of the SX Phe stars in globular clusters have $P < 0.10$ days. However, since there is some overlap in the period range

¹ Based on observations collected at ESO, La Silla, Chile, Proposal 68.A-0281

² INAF-Osservatorio Astronomico di Brera, Via E. Bianchi 46, I-23807 Merate (LC), Italy

³ INAF-Osservatorio Astronomico di Bologna, Via Ranzani 1, I-40127 Bologna, Italy

⁴ INAF-Osservatorio Astronomico di Padova, Vicolo dell'Osservatorio 5, I-35122 Padova, Italy

⁵ Current address: Observatoire de Genève, 51 ch. des Maillettes, CH-1290 Versoix, Switzerland

⁶ Department of Astronomy, University of Michigan, 821 Denison Building, Ann Arbor, MI 48109-1090

⁷ Joint Astronomy Centre, 660 N. A'ohoku Place, University Park, Hilo, HI 96720, USA

spanned by the two types of variables, disentangling HADS from SX Phe stars may not be an easy task if no details about the metallicity are known⁸. In this respect, it is appropriate to use the SX Phe term to identify the short-period Pop. II variables found in globular clusters. We will adopt this name also in the case of Fornax, since the range of metal abundance observed in Fornax is $-2.2 < [\text{Fe}/\text{H}] < -0.7$ (Saviane et al. 2000; Pont et al. 2004; Battaglia et al. 2006; Gullieuszik et al. 2007; Coleman & de Jong 2008), so that all the short-period pulsating stars in this galaxy are more similar to the SX Phe stars according to the nomenclature scheme described above. However, we note that in a different environment such as the Fornax dSph galaxy the criteria used in the Milky Way may not be adequate to describe the mixture of stars having such different ages and metallicities.

2. OBSERVATIONS AND DATA REDUCTIONS

2.1. Observations

Observations of one field north of the center of Fornax dSph, centered at $\alpha = 2^{\text{h}}39^{\text{m}}59^{\text{s}}$, $\delta = -34^{\circ}10'00''$ (J2000.0), were obtained using the Wide-Field Imager (WFI) at the 2.2 m ESO/MPI telescope. The mosaic is composed of 8 EEV “CCD 44” type CCDs, each having 2048×4096 pixels. The pixel scale is $0.238'' \text{ pixel}^{-1}$ yielding a field-of-view of $34 \times 33 \text{ arcmin}^2$.

The Fornax field was observed on three consecutive nights (Nov. 8–11, 2001) for 6.2, 7.5, and 7.7 hours, respectively. To maximize the stability of differential photometry of variable stars, no dithering was applied. Our goals were to obtain data in a two-color system and at least one very dense time series. We noted that the passband of the ESO842 *B*-filter is larger than that of the ESO 843 *V*-filter; hence, the former filter was more suitable to reach the desired signal-to-noise ratio in a short time, an observational constraint posed by the expected very short periods. Moreover, the amplitudes of the SX Phe stars are expected to be slightly larger in *B*-light than in *V*-light. Hence, 3–4 consecutive images were taken in *B*-light (700 s each), followed by a single exposure in *V* (1000 s). We collected 61 images in *B* and 16 in *V* across the 3 nights. This strategy ensured the dense *B* time series necessary to perform a reliable frequency analysis, and allowed us to obtain the mean brightness and amplitude values in a two-color system and reliably place the variable stars on the Fornax dSph color-magnitude diagram (CMD).

The sky conditions were generally stable and photometric, especially on the third night used as our reference for absolute photometric calibration. The standard fields Ru 149, Ru 152, and T Phe (see Landolt 1992) were observed to this purpose in all CCDs, with typical exposure times 300–350 s in *B* and 450–500 s in *V*. The seeing conditions varied from $1.0''$ to $1.8''$.

2.2. Data Reduction

⁸ In the past, it was quite common to use the term “Dwarf Cepheids” to identify both HADS and SX Phe stars, since their light curves are reminding those of the Classical Cepheids. This term has an unclear meaning in an astrophysical context, since it groups stars belonging to different populations, and has not been used here.

TABLE 1
CALIBRATION COEFFICIENTS FOR THE WFI

CCD	z_{PB}	c_B	z_{PV}	c_V
1	24.755	0.263	24.292	-0.086
2	24.694	0.281	24.238	-0.074
3	24.692	0.254	24.227	-0.082
4	24.729	0.264	24.280	-0.073
5	24.734	0.256	24.282	-0.075
6	24.659	0.289	24.222	-0.090
7	24.674	0.257	24.223	-0.088
8	24.722	0.266	24.284	-0.090

Image reduction of the CCD mosaic data was accomplished in IRAF⁹ using standard procedures. All multi-extension images were bias-subtracted and divided by twilight flat-fields using the mosaic reduction package MSCRED (Valdes 1998). A bad-pixel mask was created, and CCD blemishes and bad columns interpolated over. This step was necessary since CCD defects significantly increase the number of false detections by the image subtraction software we used to identify variable sources (ISIS 2.1, Alard 2000).

The images were astrometrically calibrated using a polynomial solution computed on astrometric fields from Stone et al. (1999) to remove distortion and the photometric effects of the variable pixel area. The images were then registered onto a common distortion-free coordinate grid using stars in the USNO-A2.0 Catalogue (Monet et al. 1998). The package MSCRED was used to this purpose, along with the pipeline script package WFPRED developed by two of us (LR and EVH) at the Padua Astronomical Observatory. The multi-extension images were then split and the individual CCD images analyzed separately.

Crowded field stellar photometry was performed with the ALLFRAME package (Stetson 1994), with spatially varying point-spread functions (PSFs) independently computed for each CCD and each filter. Aperture corrections were used to match the PSF photometry to large-aperture photometry on selected reference images taken on the best photometric night, using growth-curve analysis of bright isolated stars.

The absolute calibration was derived from standard star observations on the best night. A set of linear calibration relations was computed for every CCD:

$$B = b + c_B(B - V) + z_{PB} \quad (1)$$

$$V = v + c_V(B - V) + z_{PV} \quad (2)$$

where b and v are the instrumental magnitudes normalized to 1 s exposure and corrected for atmospheric extinction. The color terms and zero-points of the calibration are given in Table 1. These relations were used to calibrate, independently for each CCD, the mean instrumental PSF-fitting magnitudes, after appropriate aperture correction, and the individual data points in the light curves. The zero-point uncertainty on the cali-

⁹ The Image Reduction and Analysis Facility (IRAF) software is provided by the National Optical Astronomy Observatories (NOAO), which is operated by the Association of Universities for Research in Astronomy (AURA), Inc., under contract to the National Science Foundation.

brated magnitudes is of the order 0.04 mag in B and V , including the uncertainties on the calibration, the aperture corrections, and the residual zero-point variations within each CCD.

2.3. Variable star search

Variable stars were identified by applying the Image Subtraction Technique. We used the package ISIS 2.1 (Alard 2000) which was run on the B and V image sequences independently. This package identifies variable sources by direct comparison of the time-sequence of images, and is specifically designed to allow the detection of faint, small amplitude variables in crowded fields. Each CCD of the WFI mosaic was analyzed individually. The B and V catalogs of the candidate variables were cross-identified and conservative selection criteria were applied to the objects displaying variability flags. On average we detected about 300–400 candidate variables in each of the 8 CCDs of the WFI mosaic. The reference frames produced by the Image Subtraction were matched to the astrometric reference frames during the photometric reduction process. Instrumental b and v time series of the candidate variables were obtained by matching the ISIS catalogs and the ALLFRAME photometric catalogs. In each chip we then selected a number of comparison stars (up to 12), chosen amongst the most stable objects, and built differential light curves that were subsequently examined using period-search user–interactive tools (see Greco et al. 2007 and Clementini et al. 2008, in preparation, for details) in order to confirm the variability, and derive periods and type of variability of the confirmed variables. Finally, the instrumental ALLFRAME photometry of the confirmed variables was transformed to the standard Johnson-Cousins photometric system using the equations derived in the calibration process.

We have identified an extraordinary large number of bona fide variable stars of different types in our collection of time series of candidate variables (about 2500 in total). They include: several hundreds RR Lyr stars, 85 SX Phe stars, many eclipsing binaries, and a number of variables with periods longer than about 1.0 days (likely anomalous and Population II Cepheids). Figure 1 shows the CMD of the Fornax dSph obtained from the present data, with the SX Phe stars and a sub-sample of the RR Lyr variables shown as circles and squares, respectively. The isochrones from Girardi et al. (2000, solid lines) bracket the bulk of the Fornax SX Phe stars. The mean ridge line of the Galactic globular cluster M3 (Ferraro et al. 1997, dashed line) provides a good fit of the old ($t > 10$ Gyr) stellar component producing the Fornax RR Lyrae stars. We have adopted the following parameters for M3: $[Fe/H] = -1.66 \pm 0.06$ (Zinn & West 1984), $E(B - V) = 0.01$ (Harris 2003), and a dereddened distance modulus of $(m - M)_0 = 15.04$ mag, as inferred from the average magnitude of the cluster RR Lyrae stars (Corwin & Carney 2001). Preliminary results on the RR Lyr stars were presented in Greco et al. (2005). In the present paper we will focus on the SX Phe stars. A more detailed analysis of the Fornax RR Lyr stars and of the other types of variables will be presented in the following papers of this series.

3. THE FORNAX SX PHOENICIS STAR SAMPLE

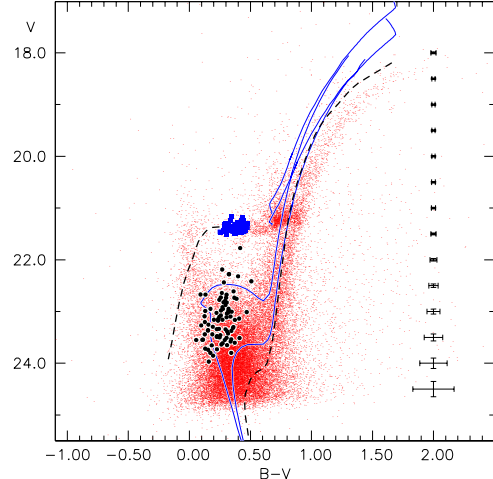


FIG. 1.— Color-magnitude diagram of the Fornax field (only data in one of the CCDs of the WFI mosaic, CCD#6, with ALLFRAME errors less than 0.06 mag have been plotted for clarity), with superimposed our total sample of SX Phe stars (85 objects, *black dots*) together with a sub-sample of 80 RR Lyr stars (marked by *blue squares*). The error bars represent $\pm 3\sigma$ typical uncertainties of the mean magnitudes and colors at different magnitude levels. The solid lines are the isochrones from Girardi et al. (2000), with $Z = 0.001$ and ages 2.2 and 7.1 Gyr, plotted to show the positions of the turnoff points at different ages. The dashed black line is the mean ridge line of the Galactic globular cluster M3 (Ferraro et al. 1997). See the electronic edition of the journal for a color version of this figure.

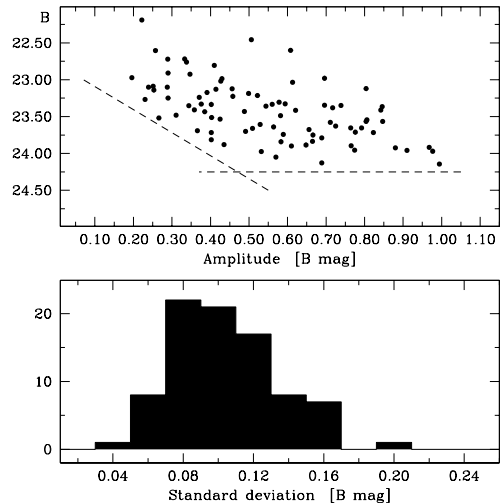


FIG. 2.— Precision and depth of our survey at the SX Phe stars magnitude level. *Upper panel:* B magnitudes of the detected SX Phe stars vs. the amplitude of their light variation. *Lower panel:* Distribution of the standard deviation showing the measurement precision for variable stars in the 22.5–24.0 mag range.

The analysis of the time series described in the previous section allowed us to identify 85 SX Phe variables according to the criteria we describe in this section. It should be pointed out that the identification of short-period variables is, in general, more difficult than, for instance, the detection of RR Lyr stars. Firstly, they are intrinsically much fainter than the RR Lyr stars (indeed,

TABLE 2
IDENTIFICATION AND PROPERTIES OF THE FORNAX DSPH SX PHE STARS

Name ^a	α (2000.0)	δ (2000.0)	Period (days)	Epoch (T_{\max}) (HJD-2452222)	$\langle B \rangle$	A_B	$\langle B \rangle - \langle V \rangle$	Type ^b
8_V9899	2 41 14.2	-34 23 02.7	0.04619	0.266	23.98	0.53	-	F
7_V8618	2 40 20.2	-34 23 58.6	0.04917	0.170	24.14	0.99	0.34	SL
2_V3796	2 40 12.1	-34 09 07.3	0.05137	0.253	23.96	0.77	0.23	F
5_V6170	2 38 51.9	-34 24 46.7	0.05326	0.289	23.27	0.23	0.32	FO
5_V15474	2 39 02.6	-34 20 26.4	0.05338	0.238	23.66	0.51	0.36	F
5_V16343	2 38 42.1	-34 20 00.3	0.05339	0.256	23.92	0.88	0.41	F
7_V5215	2 40 12.2	-34 25 23.7	0.05413	0.262	23.43	0.49	0.27	FO
2_V16907	2 40 18.5	-34 01 19.6	0.05490	0.309	23.88	0.44	0.34	F

NOTE. — Units of right ascension are hours, minutes, and seconds, and units of declination are degrees, arcminutes, and arcseconds. Table 2 is published in its entirety in the electronic edition of the *Astrophysical Journal*. A portion is shown here for guidance regarding its form and content.

^a Variable stars are ordered by increasing period, the first digit of the ID gives the number of the CCD in the WFI mosaic, the second part is the DAOPHOT identifier.

^b F: fundamental radial-mode pulsator; FO: first overtone radial-mode pulsator; SL: subluminoous variable.

TABLE 3
 B, V PHOTOMETRY OF THE FORNAX DSPH SX PHE STARS

Star 8_V9899 - P=0.04619			
HJD (-2452222)	V	HJD (-2452222)	B
0.578	23.89	0.704	23.76
0.591	23.97	0.795	23.79
0.634	23.52	1.629	23.75
0.644	23.77	1.714	23.70
0.669	24.07	1.800	23.38
0.678	23.93	2.556	23.91
0.689	23.82	2.643	23.76

NOTE. — Table 3 is published in its entirety in the electronic edition of the *Astrophysical Journal*. A portion is shown here for guidance regarding its form and content.

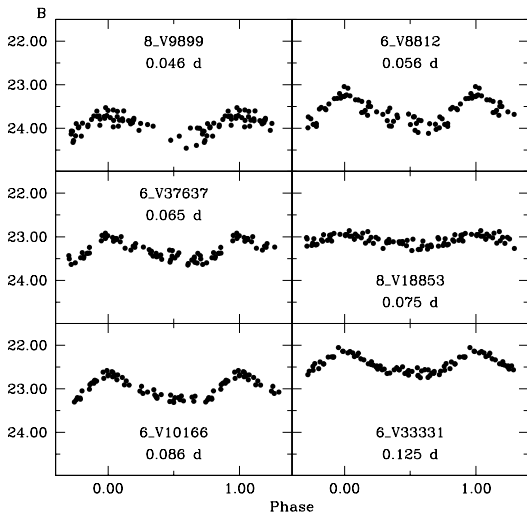


FIG. 3.— Examples of B light-curves of SX Phe stars in Fornax. Note how the mean brightness increases with increasing pulsation period. Light curves of all variable stars are available in the electronic edition of the journal.

only the use of the image subtraction permitted us to be successful in Fornax), and secondly, while the about half-a-day periodicity makes the RR Lyr variables clearly stand out just looking at the intranight light curves, this is not the case for the SX Phe stars, whose shorter periods, smaller amplitudes and the fewer number of points per cycle make the regular variability hardly discernible by simply plotting the points sequence. Therefore, we performed the frequency analysis of the data by applying a least-squares iterative sine-wave method (Vaniček 1971) both to the whole 3-nights time series and to the measurements of each individual night separately. The comparison of the power spectra obtained in the two different ways allowed us to reject a number of spurious candidates, i.e., stars for which the scatter in just one night (or in a part of it) mimicked an apparent variability. The fit of such an apparent variability can produce a false peak in the power spectrum owing to the limited time coverage of our data. To ensure the best quality of our sample, we thus accepted as bona-fide SX Phe stars only candidates whose power spectra showed the presence of a peak at the same frequency value in all the three nights (see Dell’Arciprete 2006 for a detailed description of the full procedure).

Figure 2 shows the depth of our survey of the Fornax field at the magnitude level of the SX Phe stars. The faintest SX Phe stars in our sample have $\langle B \rangle = 24.0$ mag. At this brightness level the smallest detectable amplitudes are of about 0.5 mag, but they become smaller with increasing the star’s brightness and a 0.25 mag variability could be detected in stars with $\langle B \rangle > 23.5$ mag. In particular, small amplitude (< 0.10 mag) pulsators would be detectable only if they have $B < 23.0$, whilst almost all the SX Phe variables in Fornax are fainter than $B = 23.0$. The 700 s exposure time also makes very difficult the detection of small amplitude, very-short period pulsators.

Figure 3 shows examples of the B, V light curves of the Fornax SX Phe stars we obtained at the end of the whole procedure. The full atlas of light curves is published in the electronic edition of the journal. Identification (IDs and coordinates) and parameters of the light curves (period, time of maximum light, mean $\langle B \rangle$ magnitude and $\langle B \rangle - \langle V \rangle$ color, and B -amplitude $-A_B-$) are provided in Table 2, which is published in its entirety in the electronic edition of the journal. They were calculated using

cosine-series truncated at the last significant term (usually the first harmonic, in exceptional cases the second or the third) and a least-squares fit. Error bars on the $\langle B \rangle$ and $\langle V \rangle$ magnitudes are of 0.01 and 0.04 mag, respectively. Errors in the periods range from 2×10^{-5} to 7×10^{-5} days. The last column of Table 2 gives the pulsation characteristics. They were identified following the procedures described in Section 4. The B and V photometry of all the SX Phe stars we identified in Fornax is provided in Table 3, available in electronic form in the electronic edition of the journal.

The lower panel of Fig. 2 shows the distribution of the standard deviations of the B light curve best fit models, indicating a median precision of 0.10 mag. We also note that in seven cases only (8_V28121, 3_V6718, 6_V39151, 8_V1625, 8_V9899, 6_V14592, and 8_V20859) the fit of the V -data was unsuccessful due to the incomplete phase coverage. As usual for single-site observations, the frequency detections can be affected by the ± 1 days $^{-1}$ alias ambiguity. However, this has negligible effects on the $\log P$ values for $P \leq 0.10$ days; for $P \geq 0.11$ days the alias ambiguity can shift the $\log P$ values by -0.05 or $+0.05$ only.

The high amplitudes (>0.20 mag) and the short periods ($P \leq 0.08$ days in 83% of the cases) of the stars in the Fornax sample rule out a significant contamination from rotational variables and binaries, which are expected to show smaller amplitudes and longer periods. We stress that the 85 SX Phe variables make the Fornax dSph galaxy unique in richness of such high-amplitude, short-period pulsators. The globular clusters ω Cen (Olech et al. 2005) and M55 (Pych et al. 2001) are also rich in SX Phe stars, but most of them have amplitudes smaller than 0.10 mag and seem to pulsate in nonradial modes.

In CCD6 the globular cluster Fornax 3 (For 3) is resolved into stars, at least in its outer regions, where several RR Lyr stars were identified. Two SX Phe stars were found in the outskirts of For 3, namely 6_V40765 and 6_V38403. Their vicinity to For 3 suggests that they could be cluster members. On the other hand, star 7_V22094 is at least 1.0 mag brighter than other SX Phe stars of similar period. Assuming they also have same absolute magnitude, the 1.0 mag difference implies a ratio of 0.6 between the distances. Therefore, 7_V22094 possibly does not belong to the Fornax galaxy and it could be a star in the halo of the Milky Way.

4. CHARACTERISTICS OF THE FORNAX SX PHE STARS

As shown in Fig. 1, most of the SX Phe stars lie at $22.4 < V < 23.6$ mag, hence from 1.0 to 2.2 mag fainter than the well-defined central part of the galaxy horizontal branch, which is filled by the RR Lyr stars. Their $B - V$ indices span about 0.40 mag, but 84% of the SX Phe stars have $B - V$ colors in the range from 0.10 to 0.35 mag. Taking into account the uncertainties in the $B - V$ values from the least-squares fit (± 0.04 mag) and from the calibration procedures (± 0.04 mag), the Fornax instability strip appears to be slightly larger than that of the Milky Way. We note that the Galactic HADS and SX Phe stars are located in the $(b - y)_0 = 0.13 - 0.25$ mag interval (McNamara 2000), which translates into a $B - V$ range narrower than 0.20 mag.

Due to the larger number of datapoints, our $\langle B \rangle$ magni-

tudes are more accurate than the $\langle V \rangle$ ones and therefore more suitable to study the characteristics of the Fornax SX Phe stars. The properties of SX Phe stars in Fornax are summarized in Fig. 4. Panel *a* shows the mean $\langle B \rangle$ apparent magnitudes of the Fornax SX Phe stars plotted versus observed periods. The least-squares linear fit over 84 stars (excluding star 7_V22094) is shown by the solid line; its standard deviation is 0.29 mag. This dispersion is too large to be accounted for by geometrical effect. If we consider the tidal radius of Fornax, the difference in apparent magnitude between stars with same absolute magnitude located at opposite sides of the galaxy does not exceed 0.10 mag. On the other hand, since the RR Lyr stars are all grouped in the expected narrow range of the horizontal branch, we can also exclude the existence of regions with different absorption in Fornax. Regarding possible observational errors or variability misidentification, the SX Phe stars define very clearly the instability strip below the horizontal branch.

The spread of the B magnitudes is 1.4 mag in the narrow $\log P$ interval from -1.15 to -1.05 (Fig. 4, panel *a*). Such spread is as large as the total range spanned by B magnitudes all along the observed periods. It follows that the dispersion of the points must be intrinsic to the SX Phe stars. The same conclusion can be drawn when comparing the mean $\langle V \rangle$ magnitudes and observed periods of our SX Phe sample to the Period-Luminosity ($P - L$) relations of McNamara et al. (2004). We adopt $E_{B-V} = +0.02$ mag and $m - M = 20.72$ mag (dereddened value, Greco et al. 2005; Rizzi et al. 2007) and $[\text{Fe}/\text{H}] \approx -1$ dex (average metallicity of the Fornax stars, Saviane et al. 2000; Battaglia et al. 2006). This comparison is shown in panel *b* of Fig. 4, where the solid line is the $P - L$ relation of McNamara et al. (2004) which is valid for $[\text{Fe}/\text{H}] > -1.5$ dex. If we adopt instead $[\text{Fe}/\text{H}] = -2.0$ dex, and use the second $P - L$ relation given by McNamara et al. (2004), which is valid for $[\text{Fe}/\text{H}] < -1.5$ dex, we obtain a parallel line shifted by only 0.06 mag toward fainter magnitudes.

Notwithstanding the large dispersion along the y -axis in panels *a* and *b* of Fig. 4, it is quite evident that the Fornax SX Phe variables follow a $P - L$ relation, since stars with longer periods are also brighter (see also Fig. 3). In the following subsections we will investigate the physical reasons that may cause the observed scatter of the B magnitudes at a given period.

4.1. Fundamental-mode and first-overtone pulsators

When examining panels *a* and *b* of Fig. 4, it appears that several stars are much brighter than expected from the $P - L$ relations and even more are much fainter. To provide a quantitative analysis of the different groups of SX Phe stars that may be present in our Fornax sample, we calculated the B^* values defined as $B^* = B + 2.90 \log P_F$, where P_F is the period of the fundamental radial mode. Here, the slope is that given by McNamara et al. (2004). By using the observed periods, we precisely evidenced 17 stars being 0.35 mag (or more) brighter than the value predicted by the $P - L$ relations. We note that the aliasing effect (± 1 days $^{-1}$) will produce a shift of only 0.10 mag at $\log P = -1.115$ days, unable to account for the bright magnitudes observed for these 17 objects.

The presence of such brighter stars in our SX Phe

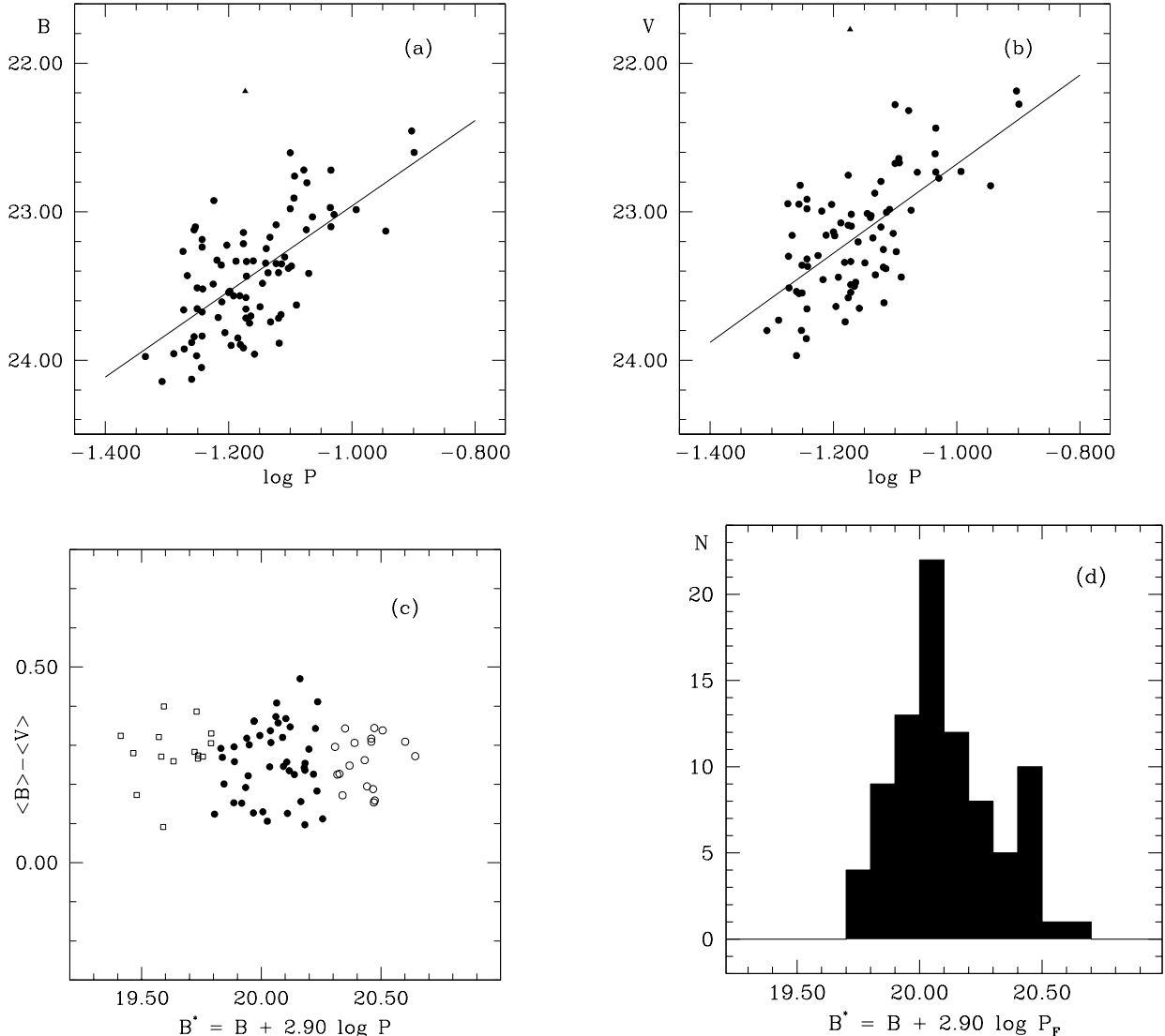


FIG. 4.— Properties of the Fornax SX Phe variables. *Panel a*: Mean $\langle B \rangle$ magnitudes plotted against observed periods. The solid line is the least-squares fit calculated from these values excluding star 7_V22094 (filled triangle) which does not belong to the Fornax dSph; *Panel b*: Mean $\langle V \rangle$ magnitudes plotted against observed periods. The solid line is the $P-L$ relation by McNamara et al. (2004) which was superposed to the data assuming for Fornax a reddened distance modulus of 20.78 mag; *Panel c*: B^* -magnitudes plotted against color indices (see text). Filled circles are stars pulsating in the fundamental radial mode; open squares are stars pulsating in the first overtone; open circles indicate the group of subluminal stars; *Panel d*: Distribution of the B^* -magnitudes.

sample can be explained by a different mode of pulsation. First-overtone pulsation has been attributed to stars too bright for the observed periods both in other galaxies (Carina, Mateo et al. 1998 and Poretti 1999a; LMC, McNamara et al. 2007) and in globular clusters (ω Cen, Olech et al. 2005; M55, Pych et al. 2001). Indeed, the fundamental period of a SX Phe star pulsating in the first-overtone (FO) mode will be 1.290 times longer than the observed one, according to the period ratio typical of the SX Phe pulsators ($P_{FO}/P_F = 0.775$, Poretti et al. 2005). Therefore, the FO-star has to be shifted rightward by +0.111 in the the $\log P - B, V$ planes, in which the fundamental periods have to be plotted on the abscissae. Assuming a slope value of the $P-L$ relations in the range from -2.90 to -3.70 , the period shift caused by the different pulsation mode corresponds to a brightening of

0.32–0.40 mag.

Similarly to what usually done in other stellar systems, we assume that the 17 stars identified by means of the procedure described above (see panel *c* of Fig. 4 for the 15 stars having reliable color indices) are FO-pulsators and calculate their F-mode periods as $\log P_F = \log P + 0.111$. This identification, though arbitrary, allows us to improve the quality of the fit, by obtaining a well-mixed group composed of “fundamentalized” first-overtone and fundamental-mode pulsators.

4.2. The subluminal variables

The identification of the brighter stars as first-overtone pulsators strongly reduces the scatter above the $P-L$ relations. However, the most remarkable feature in the $\log P - B, V$ planes still remains the presence of a large number of subluminal stars well below the $P-L$ rela-

tions toward the shortest periods, both when the $P - L$ relation is calculated from the data as in panel *a* of Fig. 4, or when it is assumed (Fig. 4, panel *b*). To explain the stars below the $P - L$ lines by a different pulsation mode we should admit that this mode has a period longer than that of the fundamental radial mode. In such a case, these stars have to be shifted leftward in the $\log P - B, V$ planes. However, periods longer than the fundamental radial one could be identified only as nonradial modes driven by gravity, but these modes are unable to produce the observed large amplitudes.

The stars below the $P - L$ lines can be better pointed out after removing the $\log P$ dependence. We calculated the distribution of the B^* magnitudes within classes with an amplitude bin of 0.10 mag (Fig. 4, panel *d*). We note that most of the subluminescent stars have $\log P \simeq -1.20$; for these values the ± 1 days $^{-1}$ ambiguity can affect the distribution in a marginal way.

The histogram shows an asymmetric distribution: there are 26 stars to the left of the central peak and 36 ones to the right. This fact cannot be ascribed to an observational bias, which should work in the opposite sense (i.e., in reducing the number of fainter stars, which are closer to the detection threshold; see Fig. 2). By using the Ashman et al. (1994) test, we considered the 21 variables having $B^* > 20.27$ as belonging to a group of subluminescent stars (Fig. 4, panel *c*). The introduction of this group of subluminescent stars accounts for the dispersions in the magnitudes of the SX Phe variables (Fig. 4, panels *a* and *b*) and for the asymmetry in their distribution (Fig. 4, panel *d*).

Figure 4, panel *c* shows that there are no differences in the average $B - V$ color of subluminescent and other stars (0.26 mag for both groups), but that the subluminescent variables span a narrower range in $B - V$ than the other stars (0.15–0.34 against 0.09–0.47 mag). The $\log P - A_B$ plot shows an abrupt decrease in the amplitudes at $\log P = -1.05$, i.e., $P = 0.09$ days (Fig. 5) regardless of the luminosity of the stars. The change in light curve properties around this period value was already observed in Galactic HADS and SX Phe stars (Poretti 2001 and references therein) and in the ω Cen SX Phe stars (Poretti 1999b).

5. $P - L$ RELATIONS FOR THE SX PHE STARS

The large sample of SX Phe stars in Fornax allows us to discuss the $P - L$ relations, both in the Fornax dSph and in other stellar systems. We evaluated the possible relevance of a color term by calculating the $P - L - C$ relations using the $\langle B \rangle - \langle V \rangle$ values and different samples (all stars, F-mode ones alone, FO-mode ones alone, subluminescent ones alone, and F-mode plus fundamentalized FO-mode ones). In all cases, the least-squares fit of the $P - L - C$ relation yields a non-significant color term. Pych et al. (2001) obtained a similar null result when trying to improve the quality of the fit by including a color term in the $P - L$ relation of stars in M55. Figure 6 shows how there is no trend in the color versus period distribution. The limited $B - V$ range (0.38 mag) and the small color excess ($E_{B-V} = +0.02$ mag) of Fornax stars do not introduce significant changes also when determining the $P - L$ relation using the extinction insensitive Wesenheit index W_V (Madore & Freedman 1991). Probably the color effect is too small to be evidenced in

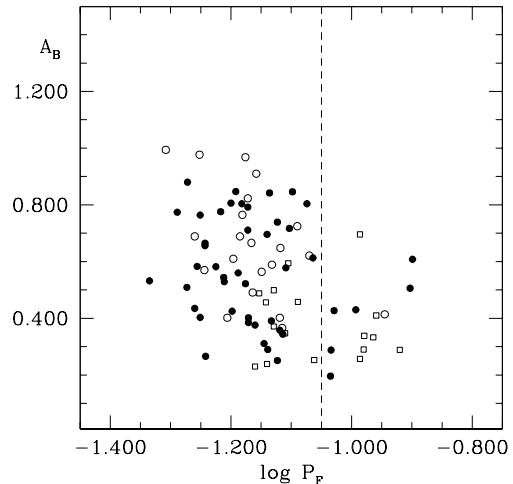


FIG. 5.— Period–amplitude diagram of the Fornax SX Phe stars: a decrease in the amplitude is observed for $\log P > -1.05$. Filled circles are F pulsators, open squares are FO pulsators, open circles are subluminescent variables.

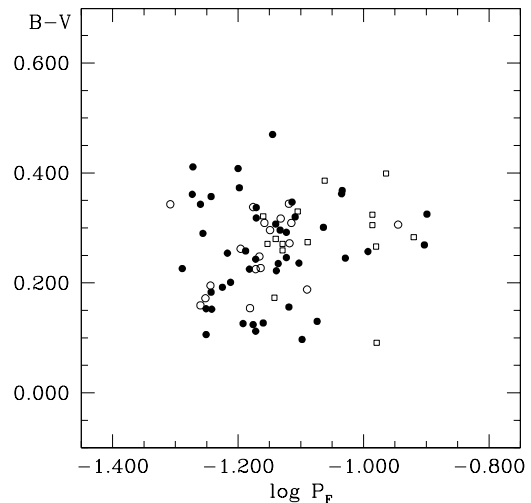


FIG. 6.— Color versus period distribution of the SX Phe stars in Fornax. Same symbols as in Fig. 5.

the short period range covered by the Fornax SX Phe stars. In this respect, we note that most of the color dependence in M55 is due to variable V21. This star has the longest period and the reddest color in the Pych et al. (2001) sample. However, its light curve shape and amplitude (only 0.04 mag) suggest that V21 could be a rotational variable.

5.1. The $P - L$ relation in Fornax

According to our identification of fundamental (46) and first overtone (17) pulsators, we have determined the $P - L$ relations. First we calculated the fundamental periods of the first-overtone pulsators assuming $P_{FO}/P_F = 0.775$. Using fundamental and “fundamentalized” periods (63 in B -light and 59 in V -light) we

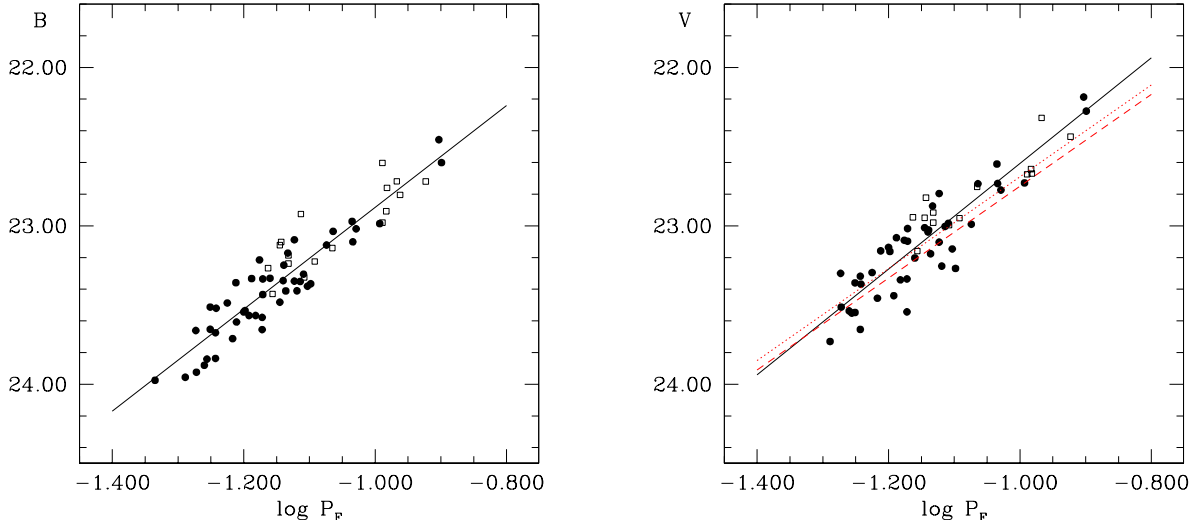


FIG. 7.— *Left panel:* $P-L$ relation of the Fornax SX Phe stars in the B -band. The solid line is the $P-L$ relation computed from the Fornax fundamental-mode (filled circles) and first-overtone (open squares) SX Phe variables. The latter were “fundamentalized” assuming $P_{FO}/P_F = 0.775$. *Right panel:* $P-L$ relation of the Fornax SX Phe stars in the V -band. The solid line is the $P-L$ relation computed from the Fornax SX Phe variables. Symbols are as in the left panel. The (red) dashed lines are the $P-L$ relations given by McNamara et al. (2004) where for Fornax we have assumed $E_{B-V} = +0.02$ mag, $m - M_V = 20.78$ mag (reddened value), and $[\text{Fe}/\text{H}] = -1.4$ dex (short dashes) or $[\text{Fe}/\text{H}] = -2.0$ dex (long dashes). See the electronic edition of the journal for a color version of this figure.

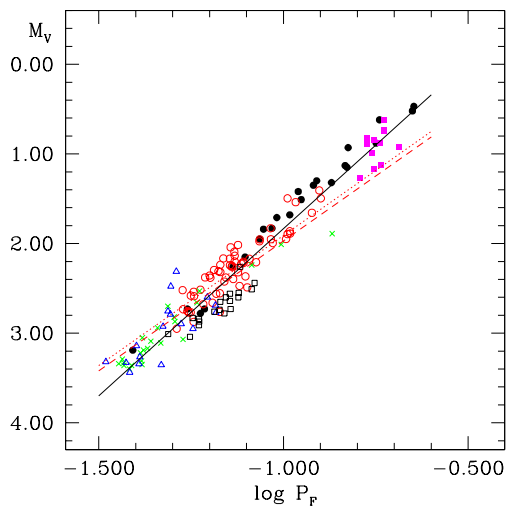


FIG. 8.— $P-L$ distribution of short-period variable stars in different stellar systems: Milky Way (black filled circles), Large Magellanic Cloud (magenta filled squares), Fornax dSph (red open circles), ω Cen (blue open triangles), M55 (green crosses), Carina dSph (black open squares). The solid line shows the $P-L$ relation given by Petersen & Hög (1998), i.e., with a slope of -3.73 , the dashed lines are the $P-L$ s obtained by McNamara et al. (2004), i.e., with a slope of -2.90 . See the electronic edition of the journal for a color version of this figure.

then obtained:

$$B = 19.66(\pm 0.19) - 3.23(\pm 0.17) \times \log P_F \quad (3)$$

and

$$V = 19.28(\pm 0.21) - 3.33(\pm 0.20) \times \log P_F \quad (4)$$

The least-squares fits are shown by solid lines in Fig. 7. Standard deviations are 0.13 mag in B and 0.15 mag in V , respectively. The slope values are different from those

assumed to calculate the B^* -magnitudes, but the subdivision into fundamental, first-overtone and subluminous pulsators does not change significantly: the main consequence of changing the slope value is a systematic shift of all the B^* -magnitudes toward brighter values.

For comparison purposes, the $P-L-[\text{Fe}/\text{H}]$ relations given by McNamara et al. (2004) are also shown in the $\log P-V$ plane of Fig. 7. The three lines are nearly coincident in the $\log P$ range covered by the Fornax sample. It is quite straightforward to use the McNamara et al. (2004) relation to calculate the distance to the Fornax galaxy. Assuming $[\text{Fe}/\text{H}] = -1.4$ dex, the 59 SX Phe stars with V light curves yield a reddened distance modulus 20.76 mag (s.d./ $\sqrt{N} = \pm 0.02$ mag), which in turn leads to $(m - M)_0 = 20.70$ mag, a value in excellent agreement with previous estimates (e.g., Buonanno et al. 1999; Saviane et al. 2000; Greco et al. 2005, 2007; Rizzi et al. 2007).

5.2. Comparison with other $P-L$ relations

There is observational evidence that short-period pulsators in a given individual stellar system cover a limited range in period and that these period ranges are very different from one system to another. The narrow period baseline hampers a reliable determination of the slope of the $P-L$ relation in a single stellar system, where stars are expected to have similar physical characteristics. We have therefore grouped all the SX Phe stars discovered so far in different stellar systems (Table 4) to span a period range as large as possible in the $\log P - M_V$ plane. To combine data from different systems, (i) we have used M_V values where available, or calculated M_V values for the short-period variables using dereddened distance moduli for the host system that are not based on the variables themselves (last column in Table 4); (ii) we have “fundamentalized” the first-overtone pulsators

TABLE 4
SX PHE AND HADS STARS IN DIFFERENT STELLAR SYSTEMS.

Stellar system	Period range (days)	SX Phe and HADS stars. Number, list and reference	Dereddened distance modulus and reference
Fornax	0.050–0.130	59 (44 F and 15 FO), Tab.2 in this paper	20.72, Rizzi et al. (2007), Greco et al. (2005)
Carina	0.045–0.075	19 (V1-V15,V17-20), in Poretti (1999a)	20.10, Dall’Ora et al. (2003)
LMC	~0.17	First 12 entries in McNamara et al. (2007), Tab. 2	18.49, McNamara et al. (2007) from RR Lyr stars
ω Cen	0.030–0.060	17 in Olech et al. (2005) (V194,V195, V199,V200,V204,V220,V225,V231,V237, V238,V250,V252,V253,NV298,NV306, NV324,NV326)	M_V values from Olech et al. (2005)
M55	0.030–0.100	23 (V16-V20,V22-V27,V31-V42) in Pych et al. (2001)	13.62, Harris (1996, 2003)
Milky Way	0.039–0.225	First 23 entries in McNamara (2000), Tab. 1	M_V values from McNamara (2000)

following the identifications provided by the authors¹⁰; (iii) we have omitted the nonradial pulsators; and (iv) all the uncertain cases were not considered, in the case of both single stars (e.g., V16 in Poretti 1999a) and of stellar systems (e.g., NGC 3201, which is affected by internal differential reddening; Piersimoni et al. 2002). Finally, we have verified that the adopted distance moduli are on the same distance scale, i.e., $(m - M)_0 = 18.50$ mag for the Large Magellanic Cloud.

The combined $P - L$ relation is shown in Fig. 8, where the SX Phe stars of ω Cen, M55, Carina, and Fornax clearly describe a linear relationship. When extending the sequence toward longer periods by adding 12 fundamental pulsators in the Large Magellanic Cloud (which are classified as δ Sct variables) and 23 pulsators in the Milky Way with $P < 0.25$ days (mostly δ Sct stars, for which $P = 0.25$ days is a safe and well established upper limit; Poretti 2001), the relation continues in a very regular and natural way. The outlier located below the sequence at $\log P = -0.87$ is variable V21 in M55. Its discrepancy with respect to other stars strengthens our hypothesis that the star is actually a rotational variable (see Sect. 5). The least-squares linear fit calculated over the total sample of stars in Fig. 8 and omitting V21 in M55 (153 stars in total) is:

$$M_V = -1.83(\pm 0.08) - 3.65(\pm 0.07) \times \log P_F \quad (5)$$

with standard deviation of 0.18 mag. The slope of -3.65 is in good agreement with first determinations obtained using short-period stars and no metallicity term, e.g., -3.725 (McNamara 2000) and -3.73 (Petersen & Hög 1998). The three $P - L$ relations are nearly coincident and for clarity only the line calculated using the Petersen & Hög (1998) parameters is shown in Fig. 8 as a solid line. We also plot in Fig. 8 the relations derived by McNamara et al. (2004), which are practically coincident with those reported by Fernie (1992) and Laney et al. (2002), and use a slope close to -2.90 . The Fornax and the Milky Way stars with $\log P > -1.0$ and the M55

stars at the shortest periods seem to fit the relation with slope of -3.73 better than those with a -2.90 slope.

We stress that when $P - L$ relations with a given slope (no matter whether -2.90 or -3.73) are used to fit periods and magnitudes of variable stars in individual clusters or galaxies, results are generally satisfactory, since their periods span too narrow ranges to put a strong constraint on the slope.

6. SUMMARY AND DISCUSSION

The detection of a large and homogenous sample of short-period variables in the Fornax dSph galaxy allowed us both to discuss the properties of SX Phe stars and to revisit their $P - L$ relation.

6.1. Origin of the subluminescent variables

The main issue of our analysis is the detection of a large scatter around the $P - L$ relation. We propose to explain such a scatter with the occurrence of different pulsation modes and the presence of a group of subluminescent stars. A mix of pulsational modes among SX Phe stars (Mateo et al. 1998; Poretti 1999a; Pych et al. 2001; Olech et al. 2005; McNamara et al. 2007) and in other pulsating stars (Red giants: Kiss & Bedding 2003, 2004; Cepheids: Udalski et al. 1999) is quite common. The subluminescent stars, shown here for the first time to be a significant population, appear to have been detectable because they exhibit high-amplitude radial pulsations and are possibly related to the complex stellar populations of Fornax. We suggest that the scatter in luminosity of short-period variable stars in Fornax has a physical rather than instrumental explanation, since observational or geometrical effects are producing a much smaller dispersion. We will attempt a preliminary discussion of possible explanations for the observed scatter, including a metallicity effect and different star-formation processes.

The metallicity effect has already been suggested by McNamara et al. (2004) to reproduce the $P - L$ relations in different environments. In Fornax the subluminescent stars, which are about 25% of the total SX Phe population, should be very metal-deficient stars. In this context, the very low metal content could explain the lack of long periods, since acoustic waves propagate faster

¹⁰ An unintentional error occurred in Fig. 10 of Pych et al. (2001). The shorter period of V35 is used instead of the longer one: if the correct period is used, the clearness of the first-overtone sequence becomes less evident.

into lighter media. If we adopt the $[\text{Fe}/\text{H}]$ dependence of -0.190 (McNamara et al. 2004), a 1.8 dex difference would be needed to produce the observed 0.35 mag luminosity difference between subluminoous variables and the bulk of SX Phe stars. Saviane et al. (2000) and Battaglia et al. (2006) report on two distinct populations, a metal-rich ($[\text{Fe}/\text{H}] > -1.3$) component and a metal-poor ($[\text{Fe}/\text{H}] < -1.3$) one. Coleman & de Jong (2008) suggest three peaks in the metallicity distribution ($[\text{Fe}/\text{H}] \simeq -1.0, -1.5, \text{ and } \leq -2.0$). Therefore, the SX Phe variables should cover the whole range of metallicities spanned by the Fornax stars and the subluminoous stars should belong to the extremely metal-poor population. However, we note that the results obtained in Sect. 5.2 suggest that the metallicity dependence is not as strong as previously inferred.

A related hypothesis is that the SX Phe stars' population in Fornax arises from different star formation processes. SX Phe stars are located in a CMD region where intermediate-age stars (the dominant population in Fornax) and old blue-stragglers may co-exist (e.g., Momany et al. 2007). The isochrones shown in Fig. 1 suggest (adopting a metallicity $Z = 0.001$) an age of ~ 3 to 6 Gyr (corresponding to a range in mass from 1.0 to 1.2 M_{\odot} at the turnoff point) for the SX Phe stars arising from a population of single intermediate-age stars. A sizable ancient population (> 10 Gyr) is also present (Saviane et al. 2000; Battaglia et al. 2006; Coleman & de Jong 2008), as demonstrated by the large number of RR Lyr stars (Greco et al. 2005) and by the fit of the position of RR Lyr stars in the CMD with the mean ridge line of the Galactic globular cluster M3, certainly older than 10 Gyr (Fig. 1). Pulsating stars resulting from the normal evolution of a single star in a finite range of ages and from the merging of a close binary system could co-exist below the horizontal branch. We can speculate that the subluminoous variables are the latter ones: after the coalescence stage, the stellar structure can be different from that produced by the normal evolution of a single intermediate-age star. Since differences in the $B - V$ indices (i.e., temperature effects) are not observed, we must infer that the blue stragglers would have a smaller radius. To explain a 0.35 mag difference, the radius of a subluminoous star should be 86% that of a normal star having same temperature. In turn, a smaller radius explains the lack of long periods. In a similar way, the blue stragglers could slightly deviate from the classical mass-luminosity relation, also taking into account that stars of different age are populating the instability strip below the horizontal branch (Fig. 1). These explanations, still tentative, seem attractive, since they would provide observational constraints on discriminating blue straggler stars in dwarf spheroidal galaxies and on theoretical models of blue stragglers' formation.

Both hypotheses need future investigations. The presence of a group of subluminoous variables may offer the possibility to use SX Phe stars as star formation tracers, since either in the case of very metal poor stars or in the case of the final stage of the evolution of close binary systems they should belong to a very old population. Spectroscopic observations of the SX Phe stars will be very useful to verify if the spread in the observed magnitudes is due to a metallicity effect as well as to study the kinematics of the different groups. The subluminoous and the

normal stars show the same spatial distribution, but we also reconsider the possibility that the subluminoous stars are related to a depth effect along the line of sight, i.e., to streams associated with the Fornax dSph galaxy. In such a case, the 0.35 mag difference implies as much as 17% in distance, which seems unlikely (Coleman & de Jong 2008). Moreover, we did not detect any subluminoous RR Lyr variable able to support a depth effect.

Have subluminoous short-period stars been observed in other environments? When modeling the SX Phe pulsating stars in ω Cen, Olech et al. (2005) found at least four cases of SX Phe stars (with amplitude from 0.03 to 0.16 mag) whose periods can be explained by masses significantly lower than expected. The SX Phe variables in Carina seem to be systematically below the $P - L$ relations in Fig. 8. This shift is small, but it could become more relevant if Carina has a distance modulus smaller than the adopted one (i.e., 20.10 mag); we note that the literature values range from 19.87 mag (Mighell 1997) to 20.19 mag (Dolphin 2002).

6.2. The slope of the $P - L$ relation

We obtained a slope value of -3.65 by combining stars in six different stellar systems. This slope differs significantly from the -2.90 value currently used, but agrees very well with previous estimates (-3.725 , McNamara 2000; -3.73 , Petersen & Hög 1998). The disagreement between the two slope values can be ascribed to different reasons. The steeper value has been (re-)obtained here as a straightforward result (Fig. 7), without considering a metallicity term. The importance of the metallicity effect is still a debated matter even in the case of Cepheids (Storm 2006). Moreover, since the metal content of individual stars in galaxies such as Carina, Fornax, and the Magellanic Clouds is still rather difficult to measure, is common procedure to use average metallicity values, which may not be very reliable. Thus neglecting the metallicity term could still be reasonable as long as accurate metal abundance of individual stars are not available. The shallower value of -2.90 is also supported by the assumption that short-period stars should be linked to Cepheids (Fernie 1992). The application of this constraint to the Milky Way stars (McNamara et al. 2007) is based on the identification of the fundamental period in low-amplitude, multiperiodic pulsators (which are the only δ Sct stars having reliable HIPPARCOS parallaxes). However, this identification is not obvious and can be made only by combining photometric and spectroscopic observations (Mantegazza 2000). A general improvement in the $P - L$ relation of SX Phe and δ Sct stars (as the reduction of the scatter and the introduction of a second term) will be possible when accurate multicolor photometry and metallicity values for individual stars in different stellar systems are available.

7. CONCLUSIONS

The intensive observation of a large part of the Fornax dSph galaxy down to 3.0 mag below the horizontal branch yielded us a suitable tool to investigate the properties of the Fornax stellar populations. The peculiar characteristics of the sample of SX Phe variables, as the group of subluminoous variables, provide useful clues on the stellar formation processes. The numerous sample of Fornax variables significantly increased the number of

SX Phe variables known in different stellar systems, allowing us the possibility to obtain a comprehensive $P-L$ relation.

We plan to determine the physical parameters of a subset of stars fitting their well defined light curves by means of theoretical pulsational models. Moreover, the Fornax project will be completed by future works on the other variables (namely, RR Lyr stars, anomalous and Pop. II Cepheids, eclipsing binaries).

ACKNOWLEDGMENTS

Part of this work has been the subject of the Laurea thesis of LDA. His supervisor and our colleague,

Prof. Laura E. Pasinetti, suddenly passed away on September 13, 2006. Several astronomers have been trained under her tutelage and we gratefully honor her memory. The authors also wish to thank H. McNamara for useful comments on a first draft of the manuscript, as well as M. Catelan and H.A. Smith for the constant support to the Fornax project. We thank the anonymous referee for comments that have helped to improve the paper. The research was funded by PRIN INAF 39/2005 (P.I. M. Tosi) and by PRIN INAF 2006 (P.I. G. Clementini).

REFERENCES

- Alard, C. 2000, *A&AS*, 144, 363
 Ashman, K.M., Bird, C.M. & Zeff, S.E., 1994, *AJ*, 108, 2348
 Battaglia, G., et al. 2006, *A&A*, 459, 423
 Buonanno, R. et al. 1999, *AJ*, 118, 1671
 Clementini, G. et al., 2006, *Mem. Soc. Astron. Italiana*, 77, 249
 Coleman, M.G., & de Jong, J.T.A. 2008, *ApJ*, in press (astro-ph/0805.1365)
 Corwin, T., M. & Carney, B., W. 2001, *AJ*, 122, 3183
 Dall’Ora, M., Ripepi, V., Caputo, F., Castellani, V., Bono, G., et al. 2003, *AJ*, 126, 197
 Dell’Arciprete, L. 2006, Laurea Thesis, Università degli Studi, Milano (in Italian)
 Dolphin, A.E. 2002, *MNRAS*, 332, 91
 Fernie, J.D., 1992 *AJ*, 103, 1647
 Ferraro, F., R., Carretta, E., Corsi, C. E., Fusi Pecci, F., Cacciari, C., Buonanno, R., Paltrinieri, B., & Hamilton, D. 1997, *A&A*, 320, 757
 Girardi, L., Bressan, A., Bertelli, G., & Chiosi, C. 2000, *A&AS*, 141, 371
 Greco C. et al. 2005, in “Resolved Stellar Populations”, D. Valls-Gabaud and M. Chavez Eds., *ASP Conf. Series*, in press (astro-ph/0507244)
 Greco, C., et al. 2007, *ApJ*, 670, 332 (Paper I)
 Gullieuszik, M., Held, E. V., Rizzi, L., Saviane, I., Momany, Y., & Ortolani, S. 2007, *A&A*, 467, 1025
 Harris, W.E. 1996, *AJ*, 112, 1487
 Harris, W.E. 2003, <http://www.physics.mcmaster.ca/Globular>
 Kiss, L.L., & Bedding, T.R. 2003, *MNRAS*, 343, L79
 Kiss, L.L., & Bedding, T.R. 2004, *MNRAS*, 347, L83
 Landolt, A. U. 1992, *AJ*, 104, 340
 Laney, C.D., Joner, M., & Schwendiman, L. 2002, in *ASP Conf. Ser.* 259, *Radial and Nonradial Pulsations as Probes of Stellar Physics*, ed. C. Aerts, T. Bedding, & J. Christensen-Dalsgaard (San Francisco: ASP), 112
 Madore, B.F., & Freedman, W.L. 1991, *PASP*, 103, 933
 Mantegazza, L. 2000, in “Delta Scuti and Related Stars”, M. Breger and M.H. Montgomery Eds., *ASP Conf. Series*, 210, 138
 Mateo, M., Harris, H., Nemeč, J., & Schombert, J. 1988, *BAAS*, 20, 717
 Mateo, M., Hurley-Keller, D., & Nemeč, J. 1998, *AJ*, 115, 1856
 Mazur, B., Krzemiński, W., & Thompson, I.B. 2003, *MNRAS*, 340, 1205
 McNamara, D.H. 2000, in “Delta Scuti and Related Stars”, M. Breger and M.H. Montgomery Eds., *ASP Conf. Series*, 210, 373
 McNamara, D.H., Rose, M.B., Brown, P.J., Ketcheson, D.I., Maxwell, J.E., Smith, K.M., & Wodey, R.C. 2004, in “Variable Stars in the Local Group”, D.W. Kurtz and K.R. Pollard Eds., *ASP Conf. Series*, 310, 525
 McNamara, D.H., Clementini, G., & Marconi, M., 2007, *AJ*, 133, 2752
 Mighell, K. 1997, *AJ*, 114, 1458
 Momany, Y., Held, E. V., Saviane, I., Zaggia, S., Rizzi, L., & Gullieuszik, M. 2007, *A&A*, 468, 973
 Monet, D.B.A., et al. 1998, *VizieR Online Data Catalog*, 1252, 0
 Nemeč, J.M., Linnell Nemeč, A.F., & Lutz, T.E. 1994, *AJ*, 108, 222
 Nemeč, J.M., Mateo, M., Burke, M., & Olszewski, E.W. 1995, *AJ*, 110, 1186
 Olech, A., Dziembowski, W. A., Pamyatnykh, A. A., Kaluzny, J., Pych, W., Schwarzenberg-Czerny, A., & Thompson, I. B. 2005, *MNRAS*, 363, 40
 Petersen, J.O., & Hög, E. 1998, *A&A*, 331, 989
 Piersimoni, A., Bono, G., & Ripepi, V. 2002, *AJ*, 124, 1528
 Cassisi, S., Salaris, M., & Castelli, F. 2004, *ApJ*, 612, 168
 Pont, F., Zinn, R., Gallart, C., Hardy, E., & Winnick, R. 2004, *AJ*, 127, 840
 Poretti, E. 1999a, *A&A*, 343, 385
 Poretti, E. 1999b, *A&A*, 346, 487
 Poretti, E. 2001, *A&A*, 371, 986
 Poretti, E. et al. 2005, *A&A*, 440, 1097
 Pych, W. et al. 2001, *A&A*, 367, 148
 Rizzi, L., Held, E. V., Saviane, I., Tully, R. B., & Gullieuszik, M. 2007, *MNRAS*, 380, 1255
 Saviane, I., Held, E. V., & Bertelli, G. 2000, *A&A*, 355, 56
 Stetson, P.B. 1994, *PASP*, 106, 250
 Stone, R. C., Pier, J. R., & Monet, D. G. 1999, *AJ*, 118, 2488
 Storm, J. 2006, in “Stellar Pulsation and Evolution”, A.R. Walker and G. Bono Eds., *Mem. Soc. Astron. Italiana*, 77, 188
 Udalski, A., Szymanski, M., Kubiak, M., Pietrzynski, G., Soszynski, I., Wozniak, P., & Zebrun, K. 1999, *AcA*, 49, 201
 Valdes, F. G. 1998, *Astronomical Data Analysis Software and Systems VII*, *ASP Conf. Ser.* 145, R. Albrecht, R. N. Hook, & H. A. Bushouse Eds., San Francisco: ASP, 7
 Vaniček, P. 1971, *Ap&SS*, 12, 10
 Zinn, R., & West, M.J. 1984, *ApJS*, 55, 45

8. ON LINE MATERIAL

Tables 2 and 3 can be requested from the first author as an ASCII and a tar file, respectively.

TABLE 2 Identification and properties of the Fornax dSph SX Phe stars

Name ^a	α (2000.0)	δ (2000.0)	Period (days)	Epoch (T_{\max}) (HJD-2452222)	$\langle B \rangle$	A_B	$\langle B \rangle - \langle V \rangle$	Type ^b
8_V9899	2 41 14.2	-34 23 02.7	0.04619	0.266	23.98	0.53	-	F
7_V8618	2 40 20.2	-34 23 58.6	0.04917	0.170	24.14	0.99	0.34	SL
2_V3796	2 40 12.1	-34 09 07.3	0.05137	0.253	23.96	0.77	0.23	F
5_V6170	2 38 51.9	-34 24 46.7	0.05326	0.289	23.27	0.23	0.32	FO
5_V15474	2 39 02.6	-34 20 26.4	0.05338	0.238	23.66	0.51	0.36	F
5_V16343	2 38 42.1	-34 20 00.3	0.05339	0.256	23.92	0.88	0.41	F
7_V5215	2 40 12.2	-34 25 23.7	0.05413	0.262	23.43	0.49	0.27	FO
2_V16907	2 40 18.5	-34 01 19.6	0.05490	0.309	23.88	0.44	0.34	F
6_V15390	2 39 51.8	-34 23 29.6	0.05493	0.229	24.13	0.69	0.16	SL
2_V4387	2 40 19.8	-34 08 49.4	0.05540	0.276	23.84	0.58	0.29	F
7_V4659	2 40 22.2	-34 25 37.7	0.05545	0.314	23.12	0.46	0.17	FO
7_V6056	2 40 28.8	-34 25 02.3	0.05569	0.230	23.10	0.24	0.28	FO
7_V7347	2 40 04.0	-34 24 30.9	0.05596	0.245	23.97	0.98	0.17	SL
7_V19493	2 39 59.2	-34 19 24.8	0.05613	0.234	23.51	0.40	0.15	F
6_V8812	2 39 31.0	-34 25 14.8	0.05616	0.322	23.65	0.76	0.11	F
3_V5563	2 39 19.6	-34 07 57.8	0.05704	0.219	24.05	0.57	0.19	SL
7_V13345	2 40 32.7	-34 21 59.7	0.05713	0.228	23.24	0.37	0.26	FO
7_V19309	2 40 14.9	-34 19 29.3	0.05716	0.323	23.19	0.50	0.27	FO
6_V44543	2 39 26.1	-34 14 37.1	0.05717	0.330	23.67	0.66	0.36	F
2_V11324	2 40 04.1	-34 04 59.9	0.05717	0.290	23.84	0.67	0.18	F
7_V33186	2 40 16.5	-34 13 29.4	0.05726	0.321	23.52	0.27	0.15	F
2_V1606	2 40 20.9	-34 10 15.5	0.05957	0.292	23.49	0.58	0.19	F
8_V1625	2 40 44.1	-34 26 45.7	0.05971	0.278	22.92	0.35	-	FO
1_V6694	2 41 06.3	-34 07 22.7	0.06041	0.325	23.33	0.59	0.33	FO
6_V40765	2 39 47.5	-34 15 53.3	0.06073	0.323	23.71	0.78	0.25	F
6_V49021	2 39 43.0	-34 12 52.0	0.06134	0.290	23.36	0.54	0.20	F
8_V28121	2 41 06.8	-34 14 48.1	0.06147	0.316	23.61	0.53	-	F
3_V6718	2 39 27.8	-34 07 16.3	0.06230	0.316	23.81	0.40	-	SL
6_V18889	2 39 42.3	-34 22 33.2	0.06265	0.266	23.23	0.46	0.27	FO
5_V26561	2 38 41.8	-34 14 36.8	0.06303	0.329	23.54	0.81	0.41	F
3_V10893	2 39 40.3	-34 04 37.1	0.06340	0.336	23.53	0.43	0.37	F
2_V7944	2 40 15.4	-34 06 54.1	0.06371	0.302	23.90	0.61	0.26	SL
6_V35797	2 39 26.7	-34 17 33.4	0.06420	0.338	23.57	0.85	0.13	F
6_V37637	2 39 53.2	-34 16 56.0	0.06481	0.276	23.33	0.56	0.26	F
6_V39151	2 39 31.6	-34 16 26.3	0.06529	0.371	23.85	0.69	-	SL
2_V4169	2 40 31.3	-34 08 55.3	0.06581	0.308	23.57	0.80	0.22	F
5_V510	2 39 07.2	-34 27 19.8	0.06596	0.330	23.90	0.76	0.15	SL
7_V2872	2 40 19.9	-34 26 22.6	0.06661	0.285	23.92	0.97	0.34	SL
7_V34972	2 40 25.8	-34 12 40.7	0.06662	0.311	23.22	0.52	0.12	F
8_V4532	2 40 41.7	-34 25 29.2	0.06668	0.344	23.14	0.25	0.39	FO
7_V22094	2 40 26.2	-34 18 17.5	0.06717	0.369	22.19	0.22	0.42	F
6_V22746	2 39 50.7	-34 21 26.7	0.06722	0.336	23.58	0.71	0.24	F
7_V15830	2 40 05.8	-34 20 58.3	0.06729	0.278	23.72	0.82	0.22	SL
2_V8650	2 40 11.9	-34 06 30.3	0.06734	0.321	23.66	0.79	0.11	F
7_V18358	2 40 07.0	-34 19 52.6	0.06739	0.312	23.33	0.40	0.32	F
8_V9427	2 40 51.0	-34 23 16.5	0.06741	0.238	23.43	0.38	0.34	F
2_V18380	2 40 11.8	-34 00 13.5	0.06817	0.435	23.75	0.67	0.25	SL
6_V44201	2 39 23.1	-34 14 44.9	0.06849	0.252	23.70	0.49	0.23	SL
7_V6259	2 40 09.5	-34 24 57.5	0.06921	0.410	23.33	0.38	0.13	F
7_V16899	2 40 35.6	-34 20 30.4	0.06945	0.394	23.96	0.91	0.31	SL
3_V17080	2 39 35.3	-33 59 20.1	0.07096	0.334	23.64	0.56	0.30	SL
6_V5831	2 39 46.1	-34 26 02.4	0.07168	0.309	23.48	0.31	0.47	F
2_V9849	2 40 23.6	-34 05 50.3	0.07240	0.386	23.35	0.70	0.31	F
6_V3640	2 39 28.4	-34 26 36.7	0.07256	0.294	23.25	0.29	0.22	F
6_V38875	2 39 29.1	-34 16 31.6	0.07316	0.409	23.41	0.84	0.23	F
6_V37380	2 39 20.6	-34 17 01.1	0.07362	0.316	23.17	0.39	0.30	F
8_V10941	2 40 42.0	-34 22 36.7	0.07373	0.352	23.74	0.59	0.32	SL
8_V18853	2 41 11.4	-34 19 02.4	0.07531	0.346	23.09	0.25	0.29	F
6_V38403	2 39 46.8	-34 16 40.7	0.07532	0.392	23.35	0.74	0.25	F
2_V881	2 40 14.6	-34 10 37.5	0.07597	0.346	23.72	0.40	0.34	SL
7_V35654	2 40 02.8	-34 12 22.7	0.07598	0.435	23.41	0.36	0.16	F
7_V9132	2 40 01.4	-34 23 46.0	0.07623	0.365	23.89	0.65	0.27	SL
8_V22313	2 41 10.9	-34 17 28.1	0.07669	0.385	23.69	0.37	0.31	SL
8_V9363	2 41 16.5	-34 23 17.0	0.07694	0.448	23.35	0.34	0.35	F
8_V7020	2 40 44.3	-34 24 21.8	0.07776	0.346	23.31	0.58	0.32	F
4_V813	2 39 08.3	-34 10 29.3	0.07887	0.341	23.38	0.72	0.24	F
6_V816	2 39 54.0	-34 27 21.4	0.07942	0.441	22.60	0.26	0.32	FO
5_V2834	2 38 59.2	-34 26 18.8	0.07952	0.353	22.98	0.70	0.31	FO
6_V33971	2 39 34.2	-34 18 08.2	0.07977	0.462	23.37	0.85	0.10	F
5_V2985	2 38 58.8	-34 26 14.7	0.08045	0.323	22.91	0.29	0.27	FO
7_V25610	2 40 27.7	-34 16 47.3	0.08064	0.327	22.76	0.34	0.09	FO

TABLE 2 continued

Name ^a	α (2000.0)	δ (2000.0)	Period (days)	Epoch (T_{\max}) (HJD-2452222)	$\langle B \rangle$	A_B	$\langle B \rangle - \langle V \rangle$	Type ^b
2_V5582	2 40 00.0	-34 08 10.6	0.08129	0.377	23.63	0.73	0.19	SL
6_V19268	2 39 52.7	-34 22 26.6	0.08365	0.305	22.72	0.33	0.40	FO
7_V1671	2 40 08.4	-34 26 52.5	0.08427	0.340	23.12	0.80	0.13	F
6_V14592	2 39 25.6	-34 23 42.2	0.08458	0.395	22.81	0.41	-	FO
8_V20859	2 41 15.2	-34 18 08.1	0.08515	0.361	23.42	0.62	-	SL
6_V10166	2 39 41.2	-34 24 53.7	0.08639	0.513	23.03	0.61	0.30	F
8_V10823	2 40 44.5	-34 22 39.9	0.09221	0.492	22.97	0.20	0.36	F
8_V30859	2 41 16.4	-34 13 30.6	0.09245	0.472	23.10	0.29	0.37	F
7_V19699	2 40 21.0	-34 19 19.2	0.09254	0.507	22.72	0.29	0.28	FO
7_V21373	2 40 05.0	-34 18 36.0	0.09345	0.495	23.02	0.43	0.25	F
7_V32007	2 40 08.5	-34 14 01.1	0.10151	0.494	22.99	0.43	0.26	F
2_V7941	2 40 30.8	-34 06 53.9	0.11348	0.541	23.13	0.41	0.31	SL
8_V33331	2 40 47.8	-34 12 20.4	0.12508	0.631	22.46	0.51	0.27	F
6_V19089	2 39 42.2	-34 22 29.8	0.12619	0.648	22.60	0.61	0.32	F

Units of right ascension are hours, minutes, and seconds, and units of declination are degrees, arcminutes, and arcseconds.

^a Variable stars are ordered by increasing period, the first digit of the ID gives the number of the CCD in the WFI mosaic, the second part is the DAOPHOT identifier.

^b F: fundamental radial-mode pulsator; FO: first overtone radial-mode pulsator; SL: subluminescent variable.

FIG. 3.— Atlas of the B and V light curves of the SX Phe discovered in the Fornax survey